as well with a large barrier (as is, in fact, the second step, tetrasilacyclobutadiene → disilyne). Thus, the fact that other Si_4H_4 minima, both singlets and high-spin states,[24] exist does not preclude the possibility of an experimentally observable T_d symmetry species Si_4H_4 (or its derivatives) which is at least somewhat kinetically stable (i.e., connected by a large barrier to other isomers). In fact, the possible existence of other stable Si_4H_4 isomers should stimulate additional experimental research directed toward the observation of other lower symmetry isomers of Si_4H_4 (or its derivatives).

Acknowledgment. This research was supported by the Director, Office of Energy Research, Office of Basic Energy Sciences, Chemical Sciences Division of the U.S. Department of Energy under Contract DE-AC03-76SF00098.

Registry No. Si_4H_4, 79517-89-8.

Quantum Mechanical Stability of Reaction Coordinate in the Unimolecular Reaction of Silanone

Akitomo Tachibana,*† Hiroyuki Fueno,† and Tokio Yamabe†,‡

Contribution from the Department of Hydrocarbon Chemistry, Faculty of Engineering, Kyoto University, Kyoto 606, Japan. *Received December 10, 1985*

Abstract: A dynamical aspect of the unimolecular dissociation reaction of silanone is analyzed. A global feature of the potential energy surface as a function of the internal coordinates of the nuclear configurations is revealed. The reaction has the negative force constant of out-of-plane vibrational mode orthogonal to the reaction coordinate. Then a new notion of the quantum mechanical stability is discussed. The dynamic features of the reaction are characterized by tunneling crossover and multistep isotope effect.

I. Introduction

Recently, theoretical studies of chemical reaction dynamics have received much attention.[1] The reason why the theoretical treatment of chemical reaction dynamics is so attractive is the existence of various rearrangement channels even for a system of a fixed number of nuclei on a single potential energy surface. In this connection, differential geometrical studies[2] and topological studies[3] of chemical reaction systems have recently been developed. The global feature of the potential energy surface as a function of the internal coordinates of the nuclear configuration is central to this direction of research, because the dynamism of the reactive flux of a chemical reaction reflects the characteristic features of the potential energy surface. The fundamental role of the IRC (intrinsic reaction coordinate)[4] as the central line of the reactive flux in the internal coordinate space has been widely demonstrated; the IRC is defined by the differential equation for a unique curvilinear reaction coordinate which connects reactant and product via a transition state on the potential energy surface. Reaction dynamics along the IRC (or meta-IRC[2] for excited-state chemical reactions) is studied by the combination of the promoting mode in the direction of the IRC and the vibrational modes in the direction orthogonal to the IRC.[1b,2,5]

In our previous work,[5] we have investigated the "stability" of the IRC in the unimolecular decomposition reaction of H_2CS and found the *negative* force constant of the out-of-plane vibrational mode orthogonal to the IRC in the early stage of the reaction. This shows that the motion of the representative particle on the IRC becomes unstable in the direction of the out-of-plane vibrational mode. This will broaden the area accessible for reactive flux to pass through the transition state. The problem of reaction coordinate instability has recently been observed in the literature from various viewpoints: in terms of the topology of potential energy surfaces,[3a] in terms of the statistical mechanics and symmetry properties of reaction systems,[4b-d] and in terms of the intrinsic field theory of environment effects.[2c]

In the present paper, we shall study the *quantum mechanical* treatment of the vibrational motions orthogonal to the IRC. Remarkably, the zero-point energy may be *negative* on the IRC. This is called the *quantum mechanical instability* of the reaction coordinate. The dynamical aspect of the new notion of the quantum mechanical stability is discussed. The relationship with the "classical" stability criterion as studied in our previous work[5] is also shown. In order to clarify the present treatment, we shall examine the unimolecular decomposition reaction of silanone,

$$H_2SiO \rightarrow H_2 + SiO \qquad (I.1)$$

and its isotope effects, as compared with the well-known corresponding reaction of H_2CO and H_2CS.[5,6] Silanone itself has recently been identified by experiment,[7] but the reaction dynamics

† Also associated with the Division of Molecular Engineering, Graduate School of Engineering, Kyoto University, Kyoto 606, Japan.

‡ Also associated with the Institute for Fundamental Chemistry, 15 Morimoto-cho, Shimogamo, Sakyo-ku, Kyoto 606, Japan.

(1) (a) *Modern Theoretical Chemistry*; Miller, W. H., Ed.; Plenum: New York, 1976; Vol. 1 and Vol. 2. (b) Daudel, R.; Leroy, G.; Peeters, D.; Sana, M. *Quantum Chemistry*; John Wiley and Sons: New York, 1983.

(2) (a) Tachibana, A.; Fukui, K. *Theor. Chim. Acta (Berlin)* **1978**, *49*, 321. (b) Tachibana, A.; Fukui, K. *Ibid.* **1979**, *51*, 189. (c) Tachibana, A.; Fukui, K. *Ibid.* **1979**, *51*, 275; **1980**, *57*, 81.

(3) (a) Mezey, P. G. *Theor. Chim. Acta (Berlin)* **1980**, *54*, 95. (b) Mezey, P. G. *J. Mol. Struct., THEOCHEM* **1985**, *123*, 171.

(4) (a) Fukui, K. *J. Phys. Chem.* **1970**, *74*, 4161. Fukui, K.; Kato, S.; Fujimoto, H. *J. Am. Chem. Soc.* **1975**, *97*, 1. Ishida, K.; Morokuma, K.; Komornicki, A. *J. Chem. Phys.* **1977**, *66*, 2153. (b) Miller, W. H.; Handy, N. C.; Adams, J. E. *J. Chem. Phys.* **1980**, *72*, 99. Miller, W. H. *J. Phys. Chem.* **1983**, *87*, 21, 3811. (c) Garrett, B. C.; Truhlar, D. G.; Wagner, A. F.; Dunning, T. H., Jr. *J. Chem. Phys.* **1983**, *78*, 4400. (d) Colwell, S. M. *Mol. Phys.* **1984**, *51*, 1217. Colwell, S. M.; Handy, N. C. *J. Chem. Phys.* **1985**, *82*, 1281.

(5) Tachibana, A.; Okazaki, I.; Koizumi, M.; Hori, K.; Yamabe, T. *J. Am. Chem. Soc.* **1985**, *107*, 1190.

(6) Jaffe, R. L.; Morokuma, K. *J. Chem. Phys.* **1976**, *64*, 4881. Heller, D. F.; Elert, M. L.; Gelbart, W. M. *Ibid.* **1978**, *69*, 4061. Kemper, M. J. H.; van Dijk, J. M. F.; Buck, H. M. *J. Am. Chem. Soc.* **1978**, *100*, 7841. Goddard, J. D.; Schaefer, H. F., III. *J. Chem. Phys.* **1979**, *70*, 5117. Goddard, J. D.; Yamaguchi, Y.; Schaefer, H. F., III. *Ibid.* **1981**, *75*, 3459. Ho, P.; Bamford, D. J.; Buss, R. J.; Lee, Y. T.; Moore, C. B. *Ibid.* **1982**, *76*, 3630. Moore, C. B. *Annu. Rev. Phys. Chem.* **1983**, *34*, 525. Dupuis, M.; Lester, W. A., Jr.; Lengsfield, B. H., III; Liu, B. *J. Chem. Phys.* **1983**, *79*, 6167. Goddard, J. D.; Clouthier, D. J. *Ibid.* **1982**, *76*, 5039. Clouthier, D. J.; Ramsay, D. A. *Annu. Rev. Phys. Chem.* **1983**, *34*, 31. Pope, S. A.; Hillier, I. H.; Guest, M. F. *J. Chem. Soc. Chem. Commun.* **1984**, 623.

0002-7863/86/1508-4346$01.50/0

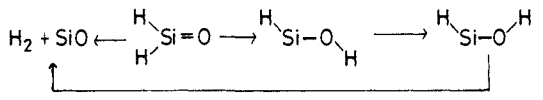

Figure 1. Reaction scheme of the unimolecular reaction of silanone.

of silanone has not been fully investigated theoretically and experimentally. So, it would be quite interesting to study the reaction coordinate of silanone.

Reaction I.1 shows quantum mechanical instability with respect to the out-of-plane vibrational mode, as will be discussed in section IIIB. The electronic process of the reaction coordinate instability will be discussed in section IIIC. Moreover, the dynamic features of reaction I.1 are characterized by (i) tunneling crossover and (ii) multistep isotope effect, as will be discussed in sections IIID and IIIE, respectively. It should be noted that the reaction dynamics of silicon compounds itself has been one of the important recent topics of current interest.[8] So, we also examine other rearrangement channels of silanone as follows:

$$H_2SiO \rightarrow \textit{trans}\text{-HSiOH} \qquad (I.2)$$

$$\textit{trans}\text{-HSiOH} \rightarrow \textit{cis}\text{-HSiOH} \qquad (I.3)$$

$$\textit{cis}\text{-HSiOH} \rightarrow H_2 + SiO \qquad (I.4)$$

II. Methods of Calculation

The molecular orbital (MO) calculations were carried out with the GAUSSIAN-80[9] program for the reactants, products, and TS's with use of the SCF method[10] with the 3-21G$^{(*)}$[11a] basis set. Geometry optimization was performed with use of the energy gradient method.[12] The electron correlation energy for each geometry was estimated by double substituted configuration interaction (CID)[13] with the 6-31G**[11b] basis set. The Davidson correction[14] was added to allow for unlinked cluster quadrupole correction (QC). The vibrational analysis and IRC were calculated in the SCF level with the HONDO[15] program by the use of the 3-21G$^{(*)}$ basis set. Moreover, configuration analysis[16] was performed.

III. Results and Discussion

(A) Geometries and Potential Energy Profiles. The reaction scheme is shown in Figure 1. The optimized geometries of reactants, products, and TSs of the reactions are shown in Figure 2. The TS is identified as the structure of a saddle point on the potential energy surface by vibrational analysis. The relative energy values of optimized geometries are shown in Figure 3.

The unimolecular dissociation reaction pathway I.1 maintains C_s symmetry. That is, the molecule has coplanarity in this reaction pathway. The out-of-plane vibrational motion gives rise to very characteristic coupling with the IRC as will be discussed later. This behavior bears a striking resemblance to the unimolecular dissociation reaction of H_2CS.[5]

The silanone may be first converted to the trans isomer by reaction I.2. Then the rearrangement channel to the cis isomer is available via reaction I.3, and the lower energy barrier is open for dissociation through reaction I.4. The unimolecular dissociation reaction of *cis*-HSiOH pathway I.4 maintains C_s symmetry and does not have the characteristic coupling with the out-of-plane vibrational motion. The most stable structure is *trans*-HSiOH, and the barrier to rearrangement is very high. This shows that the *trans*-HSiOH is thermally stable, which agrees quite well with the theoretical prediction[8a] and the experimental result.[8b]

Table I. Classification of Stability

	H_2CO	H_2CS	H_2SiO
classical	stable	unstable	unstable
quantum	stable	stable	locally unstable

(B) Quantum Mechanical Stability. Classical mechanical stability of the reaction coordinate is defined whether the energy decreases or increases in a direction orthogonal to the IRC.[5]

In this subsection, first, we shall analyze the dynamical aspect of the dissociation reaction I.1 from the viewpoint of classical mechanical stability. Figure 4 shows the frequency changes of the vibrational modes orthogonal to the reaction path, as a function of the IRC. The number on the abscissa indicates the IRC: the origin corresponds to the TS, the negative side corresponds to the reactant region, and the positive side corresponds to the product region. In this reaction, the vibrational mode corresponding to the IRC is the HSiH rocking vibration. The contribution of vibrational modes to the nuclear motion along the reaction coordinate is calculated at $s = -3.8$ in the neighborhood of the silanone equilibrium structure. The main contribution with the weight 99.97% is from the rocking mode. The frequency of the rocking vibration is 804.2 cm^{-1} at the reactant, and it is the smallest value in the vibrational modes in the plane. This is theoretically predicted by the Stable Limit Theorem.[2b] The frequency of the out-of-plane vibration is 802.2 cm^{-1} at the same point. Figure 5 shows the vibrational vectors of these normal modes.

In Figure 4 it is very characteristic that the out-of-plane vibrational mode has imaginary frequency around $s = -0.5$. The frequency has an extremum at $s = -0.5$ and it is 661.4i cm^{-1}. In this region, the *instability* of the reaction coordinate occurs. This indicates that the potential energy decreases in a direction orthogonal to the IRC around $s = -0.5$. By taking only the out-of-plane vibrational mode into consideration, the potential energy surface along the IRC may be written as follows:

$$U(s,\Delta y) = U(s) + \tfrac{1}{2}k_2(s)\Delta y^2 + \tfrac{1}{24}k_4(s)\Delta y^4;\ k_4(s) \geq 0 \qquad (III.1)$$

where s, Δy, k_2, and k_4 denote the IRC, the out-of-plane vibrational coordinate, the second-order force constant, and the fourth-order anharmonic force constant, respectively. The force constants depend parametrically on s. k_2 may change sign, but k_4 is assumed to be positive as in our previous work.[5] Figure 6 shows the potential energy profile for the direction orthogonal to the IRC at $s = -0.5$. The displacement is linear according to the displacement vector for the out-of-plane vibrational mode. The potential energy decreases for this out-of-plane nuclear motion as is expected from the imaginary frequency, that is, negative k_2. The potential energy profile is found to have a double-well structure. The minimum points are located at $\Delta y = \pm 1.8$ with stabilization energy of 8.1 kcal/mol.

The quantum mechanical nature of the reaction dynamics has been depicted by means of vibrational energy correlation.[17] The zero-point energy of the vibrational mode orthogonal to the IRC is then added to the Born–Oppenheimer potential energy along the IRC in order to determine *quantum mechanical stability* of the reaction coordinate. Hence, the Schrödinger equation is solved by means of the Runge–Kutta–Gill method, and the zero-point energy level is shown by the horizontal dotted line in Figure 6. Remarkably, the energy level is lower than the energy of the point

(7) (a) Withnall, R.; Andrews, L. *J. Am. Chem. Soc.* **1985**, *107*, 2567; *J. Phys. Chem.* **1985**, *89*, 3261. (b) Glinski, R. J.; Gole, J. L.; Dixon, D. A. *J. Am. Chem. Soc.* **1985**, *107*, 5891.

(8) (a) Kudo, T.; Nagase, S. *J. Phys. Chem.* **1984**, *88*, 2883. (b) Ismail, Z. K.; Hauge, R. H.; Fredin, L.; Kauffman, J. W.; Margrave, J. L. *J. Chem. Phys.* **1982**, *77*, 1617. (c) Schlegel, H. B. *J. Phys. Chem.* **1984**, *88*, 6254. Koehler, H.-J.; Lischka, H. *Chem. Phys. Lett.* **1984**, *112*, 33. O'Keeffe, M.; Gibbs, G. V. *J. Chem. Phys.* **1984**, *81*, 876. Jaquet, R.; Kutzelnigg, W.; staemmler, V. *Theor. Chim. Acta (Berlin)* **1980**, *54*, 205.

(9) Pople, J. A.; et al. *QCPE* **1981**, *13*, 406.

(10) Roothaan, C. C. J. *Rev. Mod. Phys.* **1951**, *23*, 69.

(11) (a) Pietro, W. J.; Francl, M. M.; Hehre, W. J.; DeFrees, D. J.; Pople, J. A.; Binkley, J. S. *J. Am. Chem. Soc.* **1982**, *104*, 5039. (b) Fancl, M. M.; Pietro, W. J.; Herhe, W. J.; Binkley, J. S.; Gordon, M. S.; DeFrees, D. J.; Pople, J. A. *J. Chem. Phys.* **1982**, *77*, 3654.

(12) Pulay, P. In *Modern Theoretical Chemistry*; Schaefer, H. F., III, Ed.; Plenum: New York, 1977; Vol. 4, Chapter 4.

(13) Seeger, R.; Krishnan, R.; Pople, J. A. *J. Chem. Phys.* **1978**, *68*, 2519.

(14) (a) Langhoff, S. R.; Davidson, E. R. *Int. J. Quantum Chem.* **1974**, *8*, 61. (b) Davidson, E. R.; Silver, D. W. *Chem. Phys. Lett.* **1978**, *52*, 403.

(15) Dupuis, M.; King, H. F. *J. Chem. Phys.* **1978**, *68*, 3998.

(16) Murrell, J. N.; Randic, M.; Williams, D. R. *Proc. R. Soc. London* **1965**, *A284*, 566. Baba, H.; Suzuki, S.; Takemura, T. *J. Chem. Phys.* **1969**, *50*, 2078. Fujimoto, H.; Kato, S.; Yamabe, S.; Fukui, K. *Ibid.* **1974**, *60*, 572. Nagase, S.; Fueno, T. *Theor. Chim. Acta (Berlin)* **1974**, *35*, 217; **1976**, *41*, 59.

(17) Latham, S. L.; McNutt, J. F.; Wyatt, R. E.; Redmon, M. J. *J. Chem. Phys.* **1978**, *69*, 3746.

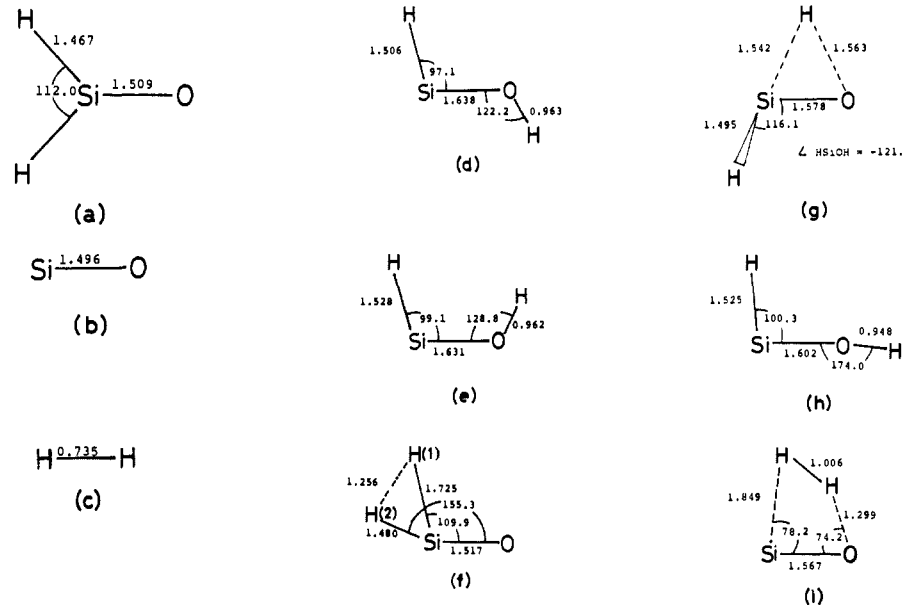

Figure 2. Optimized geometries of (a) H_2SiO, (b) SiO, (c) H_2, (d) *trans*-HSiOH, (e) *cis*-HSiOH, (f) TS of dissociation of H_2SiO, (g) TS of H_2SiO → *trans*-HSiOH, (h) TS of *trans*-HSiOH → *cis*-HSiOH, and (i) TS of dissociation of *cis*-HSiOH. Bond lengths and angles are given in Å and deg, respectively. The basis set is 3-21G(*).

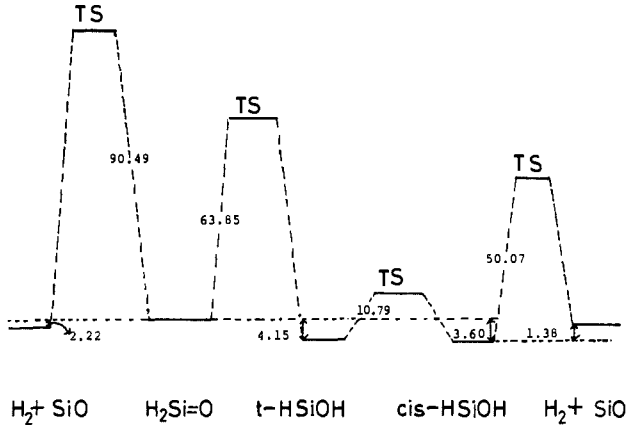

Figure 3. Relative energy values estimated by CID+Q with use of the 6-31G** basis set. The geometries are the same as in Figure 2. The unit is kcal/mol.

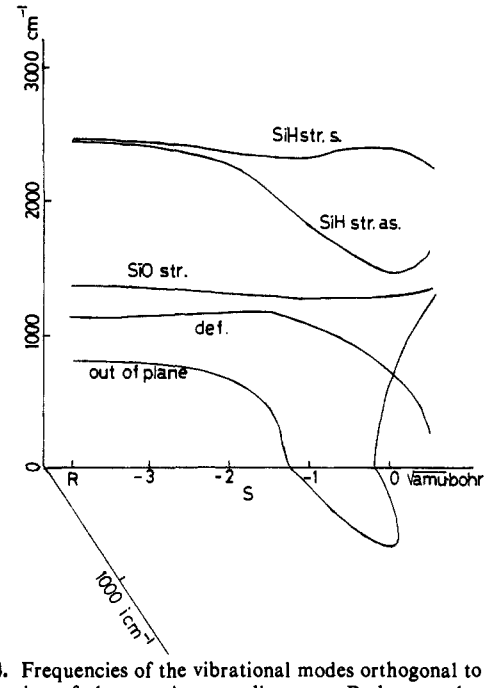

Figure 4. Frequencies of the vibrational modes orthogonal to the IRC, as a function of the reaction coordinate s. R denotes the reactant.

on the IRC. Consequently, there is a tunneling effect between two minimum points of the double-well. The difference in energy between the point on the IRC and the zero-point energy level is 6.9 kcal/mol.

The wave function profile is also shown in Figure 6. The wave function has double maxima at $\Delta y = \pm 1.8$. This indicates that the advantageous area for the reaction is broadened if we consider the out-of-plane zero-point vibrational motion along the IRC. Thus we have obtained the characteristic coupling of the out-of-plane vibrational motion with the IRC.

In Figure 7 are shown the Born–Oppenheimer potential energy profile along the IRC and the corrected potential energy profile coupled with the out-of-plane zero-point vibrational motion. The corrected potential energy is lower than the Born–Oppenheimer potential energy around $s = -0.5$. This is called the *quantum mechanical instability* of the reaction coordinate.

Quantum mechanical stability of the reaction coordinate is classified into three categories as shown in Figure 8. Typical examples are shown in Figure 9, that is, the corresponding unimolecular reactions of H_2CO and H_2CS. The stability of these reactions is summarized in Table I. The concept of stability will play an important role in the study of chemical reaction coordinates.[4]

(C) Electronic Process of Reaction Coordinate Instability. The electronic process of reaction coordinate instability is analyzed in this subsection. H_2SiO is divided into two subsystems, H_2 and SiO, at $s = -0.5$. The configuration analysis is performed, and the one-electron processes are shown in Table II. Note that the charge transfer (CT) from σ orbital of H_2 to $\pi^*_\perp$ orbital of SiO, $CT(\sigma_{H_2}-\pi^*_{SiO\perp})$, increases with increasing Δy. They are important electronic processes corresponding to the out-of-plane motion. On the other hand, $CT(\pi_{SiO\perp} - \sigma^*_{H_2})$ hardly changes with increasing Δy, because the difference of orbital energy between $\pi_{SiO\perp}$ and $\sigma^*_{H_2}$ is larger than that between σ_{H_2} and $\pi^*_{SiO\perp}$. This result indicates that the instability of reaction path is induced mainly by $CT(\sigma_{H_2} - \pi^*_{SiO\perp})$.

The electronic process of force constant matrix at stable molecular geometry has been studied by Bader.[18] In the present paper, we shall apply his analysis at the unstable molecular

(18) Bader, R. F. W. *Can. J. Chem.* **1962**, *40*, 1164.

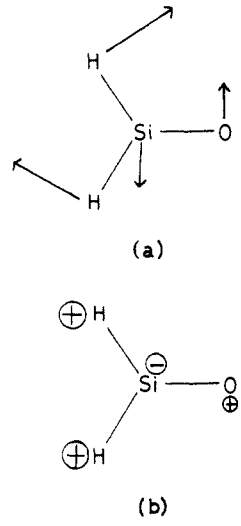

Figure 5. Vibrational modes of (a) rocking vibration and (b) out-of-plane vibration.

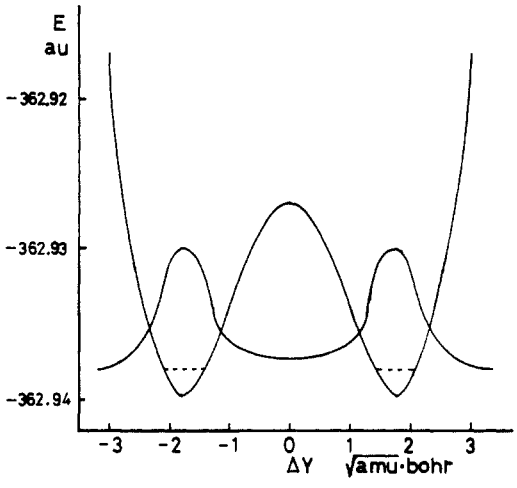

Figure 6. Potential energy profile in the direction orthogonal to the IRC at $s = -0.5$ amu$^{1/2}$·bohr and the wave function profile. The zero-point energy level of the out-of-plane vibration is shown by the horizontal dotted line.

geomery, that is, along the reaction coordinate. The force constant is constructed by two terms, the static term and the dynamic term:

$$k = k_{\text{static}} + k_{\text{dynamic}} \qquad \text{(III.2)}$$

The static term includes no electronic reorganization effect:

$$k_{\text{static}} = \frac{\partial^2 V_{\text{nn}}}{\partial Q^2} + \int \rho_{00}(1) \frac{\partial^2 V_{\text{ne}}(1)}{\partial Q^2} \, d\upsilon(1) \qquad \text{(III.3)}$$

where ρ_{00}, V_{nn}, V_{ne}, and Q denote the electron density of the ground state, the nuclear repulsion operator, the nuclear attraction operator, and the normal coordinate, respectively. The dynamic term includes the electronic reorganization effect: using the transition density ρ_{0K} between the electronic ground state and the Kth excited state, the dynamic term is represented by

$$k_{\text{dynamic}} = 2\sum_K \left| \int \rho_{0K}(1) \frac{\partial V_{\text{ne}}(1)}{\partial Q} \, d\upsilon(1) \right|^2 / (E_0 - E_K) \qquad \text{(III.4)}$$

where E_0 and E_K are the energies of the electronic ground and Kth excited states, respectively. In the present case, the out-of-plane mode has a negative force constant. Then, the dynamic term should play an important role, because it is negative definite. Indeed, the transition density corresponding to the $\sigma_{H_2} \rightarrow \pi^*_{SiO\perp}$ transition is easily accessible for the out-of-plane mode. This is schematically shown by orbital symmetry properties in Figures 10 and 11.

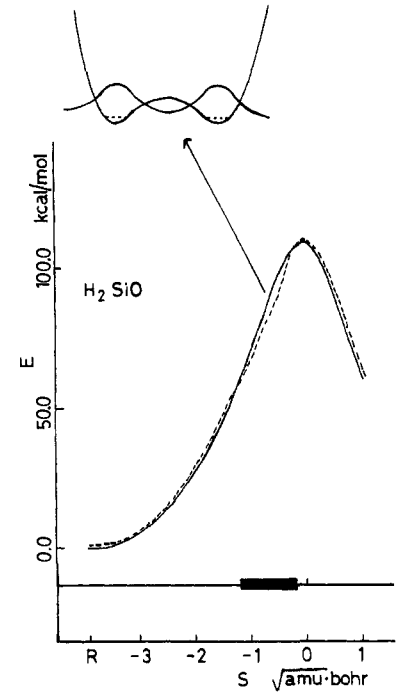

Figure 7. Born–Oppenheimer potential energy profile along the IRC (full line) and the corrected potential energy profile (dotted line). The thick part of the horizontal line represents the classically unstable region.

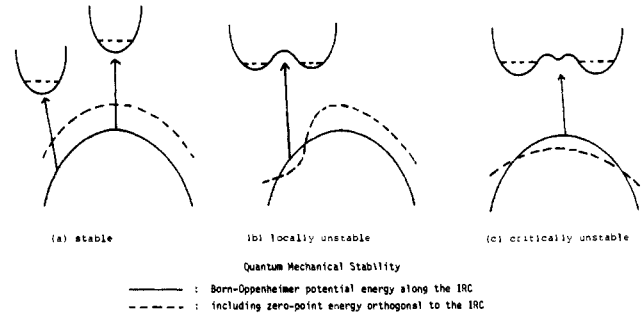

Figure 8. Quantum mechanical stability of reaction path: (a) stable, (b) locally unstable, and (c) critically unstable. The meaning of the lines is the same as in Figures 6 and 7.

Table II. Configuration Analysis of H_2SiO

Δy^a			π^*	$\pi^*_\perp$	σ^* H_2
1.8		π	0.0004	0.0013	0.0016
		$\pi_\perp$	0.0006	0.0003	0.0004
		σ	0.0142	0.0126	0.0376
	H_2	σ	0.0243	0.0156	0.0472
1.2		π	0.0001	0.0023	0.0002
		$\pi_\perp$	0.0019	0.0008	0.0004
		σ	0.0311	0.0216	0.0766
	H_2	σ	0.0511	0.0206	0.0778
0.6		π	0.0003	0.0022	0.0038
		$\pi_\perp$	0.0025	0.0017	0.0004
		σ	0.0521	0.0197	0.1228
	H_2	σ	0.0834	0.0140	0.0993
0.0		π	0.0005	0.0	0.0062
		$\pi_\perp$	0.0	0.0018	0.0
		σ	0.0605	0.0	0.1415
	H_2	σ	0.0961	0.0	0.1038

[a] Vibrational coordinate orthogonal to the IRC.

In Figure 10, we show Pearson's theory[19] that the reaction coordinate of eq I.1 should not be C_{2v} but C_s, which is in accord with our calculation. But, dynamically, the reaction coordinate

(19) Pearson, R. G. *Symmetry Rules for Chemical Reactions*; John Wiley and Sons: New York, 1976.

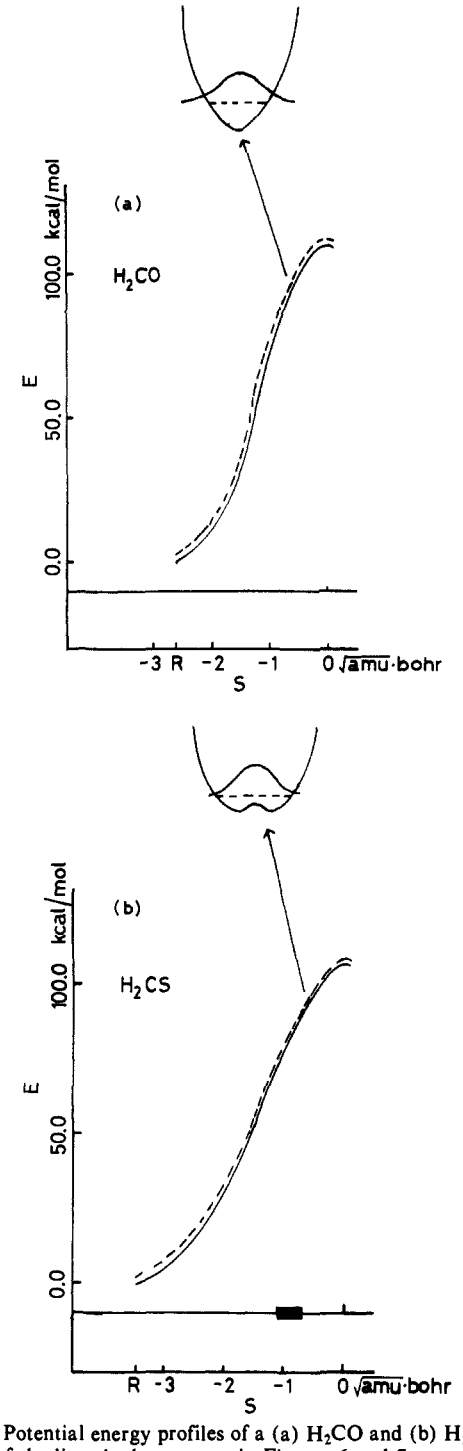

Figure 9. Potential energy profiles of a (a) H_2CO and (b) H_2CS. The meaning of the lines is the same as in Figures 6 and 7.

possesses instability. The major origin of the instability is due to the out-of-plane electronic process of $\sigma_{H_2} \rightarrow \pi^*_{SiO\perp}$ as shown in Figure 11.

It should be pointed out that we have already shown the instability of the reaction coordinate of the decomposition reaction of thioformaldehyde.[5] In the case of thioformaldehyde, the degree of instability is small as compared with the present case. The difference of the two cases is first observed in the orbital energy gap: the orbital energy gap in the electronic process $\sigma_{H_2} \rightarrow \pi^*_{CS\perp}$ is 0.541 au and the orbital energy gap in the electronic process $\sigma_{H_2} \rightarrow \pi^*_{SiO\perp}$ is 0.494 au at the instability points, respectively. This shows the latter electronic process occurs more easily. Secondly, the difference in the charge distribution is dramatic: $C^{-0.02} - S^{+0.02}$ and $Si^{+0.527} - O^{-0.527}$ at the instability points. Consequently, the distribution of the vacant $\pi^*_{SiO\perp}$ orbital at Si in SiO is larger than the distribution of the vacant $\pi^*_{CS\perp}$ orbital

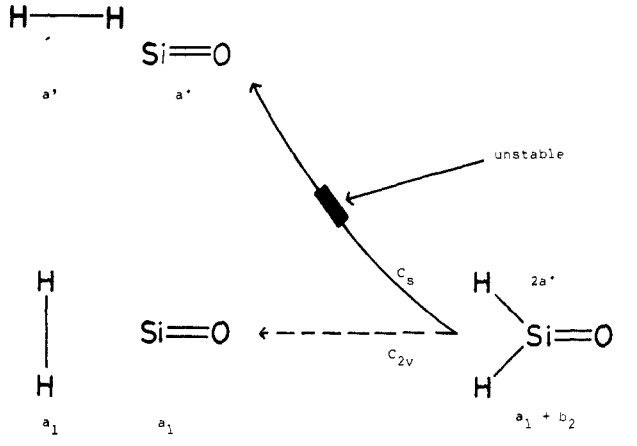

Figure 10. Orbital symmetry property of the dissociation reaction of silanone. The thick bar represents the unstable region.

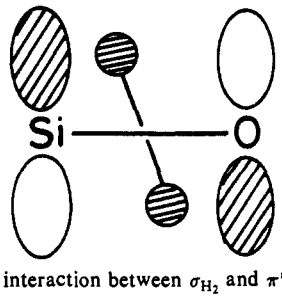

Figure 11. Orbital interaction between σ_{H_2} and $\pi^*_{SiO\perp}$.

Table III. Transmission Coefficient D of the One-Dimensional Potential Energy Barrier

	$-\ln D\ ((m_e/amu)^{1/2})$	
E (kcal/mol)	Born–Oppenheimer[a]	corrected[b]
105	2.88	3.17
100	7.53	7.13
95	12.33	11.32
90	17.28	15.79
85	22.45	20.65
80	27.80	25.95
75	33.45	31.83
70	39.48	38.25

[a] Born–Oppenheimer potential energy is used. [b] Born–Oppenheimer potential energy is corrected by zero-point energy of out-of-plane vibration.

at C in CS. Hence, the distribution of the transition density at the reaction center of reaction I.1 is greater than that of the corresponding reaction of thioformaldehyde. Thus, the two effects lead the large negative force constant of eq III.4 and hence the large instability of the present reaction I.1 as compared with the corresponding reaction of thioformaldehyde.

(D) Tunneling Crossover. The quantum mechanical instability is induced by the tunneling motion orthogonal to the IRC. This will further narrow the width of the potential barrier from the reactant to the product, and then the tunneling probability of the potential energy barrier increases. The tunneling probability is estimated by the transmission coefficient D:[20]

$$D = \exp\left(-\frac{2}{\hbar}\int_a^b |p|\, ds\right) \qquad \text{(III.5)}$$

where a and b are classical turning points, and p and s are momentum and mass-weighted reaction coordinate, respectively. The transmission coefficients were evaluated semiclassically by means of Simpson's method. The results of calculation are shown in

(20) Landau, L. D.; Lifshitz, E. M. *Quantum Mechanics*; Pergamon: London, 1965.

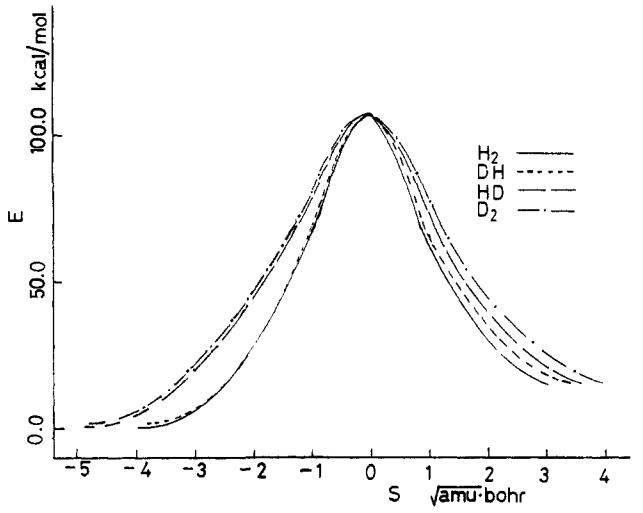

Figure 12. Isotope effect of the potential energy profile along the IRC.

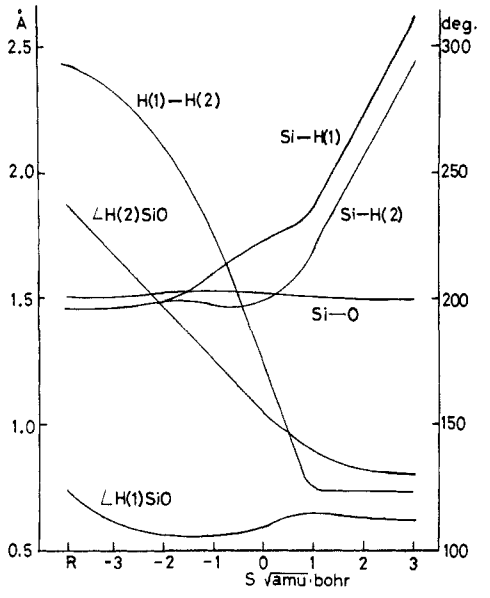

Figure 13. Changes of geometries along the IRC.

Table III. In the energy region 60 kcal/mol $\leq E \leq$ 100 kcal/mol, the tunneling probability increases greatly. Indeed, it is found from Table III that the transmission coefficients on the corrected surface in this energy region are greater than those on the adiabatic surface.

Thus, the interplay between these mutually orthogonal tunneling motions is very characteristic of this unimolecular reaction. This interplay may be called "tunneling crossover". It should be noted that the tunneling crossover occurs in a certain energy region which is determined by the quantum mechanical instability of the reaction coordinate. The incorporation of tunneling crossover to more sophisticated treatments of reaction rates[5,21] will also be quite interesting.

(E) Multistep Isotope Effect. In this subsection the isotope effect of the tunneling mechanism of the unimolecular dissociation reaction I.1 is discussed. The isotope effect of the potential energy profile along the IRC is shown in Figure 12. The characterization of hydrogen as H(1) and H(2) is defined in Figure 2f. The silanone whose H(1) is substituted by deuterium is denoted as DHSiO or "DH" for short and the silanone whose H(2) is substituted by deuterium is denoted as HDSiO or "HD" for short. The "H_2" and "D_2" are short for H_2SiO and D_2SiO, respectively.

(21) See, for example: (a) Miller, W. H. *J. Am. Chem. Soc.* **1979**, *101*, 6810. (b) Truhlar, D. G.; Isaacson, A. D.; Garrett, B. C. In *Theory of Chemical Reaction Dynamics*; Baer, M., Ed.; CRC: Boca Raton, 1985; Vol. 4, Chapter 2.

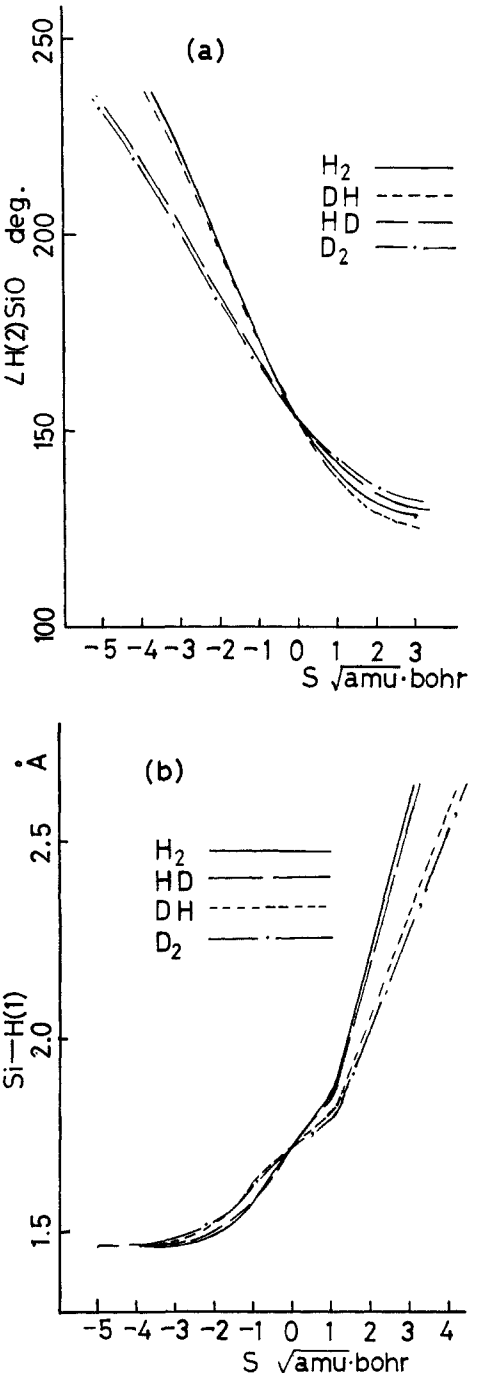

Figure 14. Isotope effect of geometry changes: (a) ∠H(2)SiO, and (b) the H(1) to Si bond length along the IRC.

Interestingly, we have two distinct groups ["H_2" and "DH"] and ["HD" and "D_2"] in the early stage of the reaction.

To investigate the mechanism of this division, the changes of geometries along the IRC are followed and are shown in Figure 13. The ∠H(2)SiO decreases greatly at first and the H(1) to Si bond lengthens secondly. Because of these two characteristic changes, "multistep isotope effect" is expected, which is the mechanism of the division.

The characteristic isotope effects are actually seen in the changes of ∠H(2)SiO and the H(1) to Si bond length as shown in Figure 14, a and b, respectively. The changes of the ∠H(2)SiO are divided into the groups ["H_2" and "DH"] and ["HD" and "D_2"]. At this step, the H(2) turns around Si and approaches H(1), and the isotope effect is observed on H(2). Also, the changes of the H(1) to Si bond length are divided into different groups, ["H_2" and "HD"] and ["DH" and "D_2"]. At this step, the H(1) to Si bond is broken, and the isotope effect is observed on H(1). The latter isotope effect overlaps the former one, but the former

Table IV. Transmission Coefficient D of DHSiO and HDSiO

E (kcal/mol)	$-\ln D$ ($(m_e/amu)^{1/2}$) DH	HD
105	3.05	3.65
100	7.95	9.54
95	12.97	15.61
90	18.21	21.90
85	23.64	28.48
80	29.27	35.34
75	35.15	42.60
70	41.41	50.96

one is greater and it controls the whole mechanism.

The isotope effect of tunneling is estimated by the transmission coefficient (eq III.5) and is shown in Table IV. Because the transmission coefficients of "DH" are always greater than those of "HD", it is easier for "DH" than "HD" to dissociate through tunneling. This verifies the mechanism of division in the isotope effect of the potential profile along the IRC (Figure 12).

IV. Concluding Remarks

In the present paper, we have studied the new aspect of the "stability" of reaction coordinate. We have emphasized the importance of quantum mechanical dynamics and the accompanying dynamical electronic processes. The mechanism of tunneling crossover is the first characteristic finding. This may be utilized as the global design of potential energy surface of chemical reaction. Secondly, the multistep isotope effect is considered the most typical feature of chemical reaction dynamics where successive rearrangement of atoms takes place. It is remarkable that if we fix SiO in the space, then the essential asymmetry is observed in the direction of dissociation between HDSiO and DHSiO as the result of the multipe isotope effect. Using this property, we may design the "dynamic" stereoselective reaction or the orientation selective transfer of isotopes in amorphous materials. Since the symmetry of molecular vibrational modes plays an important role in the reaction dynamics, the mode-selective chemistry should be the most direct application. Irradiation by laser may be most effective. The interplay between the tunneling crossover and the multistep isotope effect may then yield fruitful applications. This direction of research should be enhanced in the future.

Acknowledgment. This work was supported by a Grant-in-Aid for Scientific Research from the Ministry of Education of Japan, for which the authors express their gratitude. One of the authors, H.F., would like to thank I. Okazaki for his assistance with MO calculation. The numerical calculations were carried out at the Data Processing Center of Kyoto University and the Computer Center of the Institute for Molecular Science (IMS).

Registry No. H_2SiO, 22755-01-7.

Molecular Structure of Allyl Radical from Electron Diffraction

E. Vajda,[1a] J. Tremmel,[1a] B. Rozsondai,[1a] I. Hargittai,*[1a] A. K. Maltsev,[1b] N. D. Kagramanov,[1b] and O. M. Nefedov[1b]

Contribution from the Department of Structural Studies, Research Laboratory for Inorganic Chemistry, Hungarian Academy of Sciences, Budapest, Pf. 117, H-1431, Hungary, and the Institute of Organic Chemistry, Academy of Sciences of the USSR, Moscow 117913, USSR.
Received November 1, 1985

Abstract: The molecular structure of free allyl radical was determined from high-temperature electron diffraction augmented with mass spectrometry. The free radicals, with 75% relative abundance, were produced by vacuum pyrolysis of 1,5-hexadiene at 960 °C in the diffraction experiment. The data are consistent with a planar symmetric geometry, C–C bond length (r_g) 1.428 ± 0.013 Å, and C–C–C bond angle 124.6 ± 3.4°.

For the first time we determined the molecular structure of the free allyl radical from high-temperature electron diffraction augmented with mass spectrometry. Application of our technique[2,3] to a direct study of this unstable reactive species yielded experimental values of bond length, bond angle, and vibrational amplitudes. Our results are consistent with previous structural information on the allyl radical from ESR,[4] IR,[5] and PE[6] spectroscopy and quantum chemical calculations.[7]

The allyl radicals were generated by vacuum pyrolysis of 1,5-hexadiene[5] in a quartz reactor at about 960 °C in our electron diffraction nozzle system.[8] Electron intensity[9] and quadrupole mass spectrometric[10] measurements facilitated the choice of experimental conditions. The nozzle capillary (length of 25 mm) was wider (1 mm),[11] the vapor pressure was lower (<0.2 Torr), the primary electron beam intensities were higher (0.2 and 0.6 μA for 50 and 19 cm camera ranges, respectively), and the exposures were longer (6–10 min) than usually employed. Accordingly, the noise level of the data was also higher than usual.

The inlet system was tested in a separate mass spectrometric unit[12] to determine the temperature dependence of the vapor composition. The following relative amounts of the pyrolysis products were found at the conditions of the diffraction experiment: radical 70 mol %, propene 10 mol %, allene 15 mol %.

The electron diffraction analysis was similar to that described elsewhere.[13] Molecular intensities and radial distributions are shown in Figures 1 and 2.

The radical geometry was defined by C–C and C–H bond lenghts and C–C–C and C–C–H bond angles. Local C_{2v} symmetry was assumed for the CCH_2 moieties. A mean C–H bond length was refined assuming the methylene C–H to be shorter by 0.002 Å than the methine C–H.[7] No information could be gained on the possible deviation of the CH_2 groups from the CCC plane.

(1) (a) Hungarian Academy of Sciences. (b) Academy of Sciences of the USSR.
(2) Schultz, Gy.; Tremmel, J.; Hargittai, I.; Berecz, I.; Bohátka, S.; Kagramanov, N. D.; Maltsev, A. K.; Nefedov, O. M. *J. Mol. Struct.* **1979**, *55*, 207.
(3) Hargittai, I.; Schultz, Gy.; Tremmel, J.; Kagramanov, N. D.; Maltsev, A. K.; Nefedov, O. M. *J. Am. Chem. Soc.* **1983**, *105*, 2895.
(4) Fessenden, R. W.; Schuler, R. H. *J. Chem. Phys.* **1963**, *39*, 2147.
(5) Maltsev, A. K.; Korolev, V. A.; Nefedov, O. M. *Izv. Akad. Nauk. SSSR, Ser. Khim.* **1982**, 2415; **1984**, 555.
(6) Houle, F. A.; Beauchamp, J. L. *J. Am. Chem. Soc.* **1978**, *100*, 3290.
(7) Takada, T.; Dupuis, M. *J. Am. Chem. Soc.* **1983**, *105*, 1713.
(8) Tremmel, J.; Hargittai, I. *J. Phys. E: Sci. Instrum.* **1985**, *18*, 148.
(9) Tremmel, J.; Kolonits, M.; Hargittai, I. *J. Phys. E.: Sci. Instrum.* **1977**, *10*, 664.
(10) Hargittai, I.; Bohátka, S.; Tremmel, J.; Berecz, I. *Hung. Sci. Instrum.* **1980**, *50*, 51.
(11) Influence of gas spread due to wide nozzle opening was estimated to be negligible on the experimental amplitudes compared to other errors. See: Bartell, L. S.; Heenan, R. K.; Nagashima, M. *J. Chem. Phys.* **1983**, *78*, 236.
(12) Kagramanov, N. D.; Maltsev, A. K.; Dubinskii, M. Yu.; Nefedov, O. M. *Izv. Akad. Nauk SSSR, Ser. Khim.* **1983**, 536.
(13) Hargittai, M.; Hargittai, I. *J. Chem. Phys.* **1973**, *59*, 2513.

0002-7863/86/1508-4352$01.50/0